

RGF1 controls root meristem size through ROS signalling

<https://doi.org/10.1038/s41586-019-1819-6>

Masashi Yamada^{1,2,3}, Xinwei Han^{1,4} & Philip N. Benfey^{1*}

Received: 30 November 2017

Accepted: 22 October 2019

Published online: 4 December 2019

The stem cell niche and the size of the root meristem in plants are maintained by intercellular interactions and signalling networks involving a peptide hormone, root meristem growth factor 1 (RGF1)¹. Understanding how RGF1 regulates the development of the root meristem is essential for understanding stem cell function. Although five receptors for RGF1 have been identified^{2–4}, the downstream signalling mechanism remains unknown. Here we report a series of signalling events that follow RGF1 activity. We find that the RGF1-receptor pathway controls the distribution of reactive oxygen species (ROS) along the developmental zones of the *Arabidopsis* root. We identify a previously uncharacterized transcription factor, *RGF1-INDUCIBLE TRANSCRIPTION FACTOR 1 (RITF1)*, that has a central role in mediating RGF1 signalling. Manipulating *RITF1* expression leads to the redistribution of ROS along the root developmental zones. Changes in ROS distribution in turn enhance the stability of the PLETHORA2 protein, a master regulator of root stem cells. Our results thus clearly depict a signalling cascade that is initiated by RGF1, linking this peptide to mechanisms that regulate ROS.

Plant roots encounter varying environmental conditions and respond by altering their growth. Root growth arises through controlled cell division in the root's meristematic zone (equivalent to the transit amplifying zone in animals). After division, most cells increase their size in the elongation zone, and mature in the differentiation zone. The sizes of these developmental zones are determined by intrinsic and extrinsic signals. ROS are an intrinsic signal for establishing the size of the meristematic zone: superoxide (O_2^-) accumulates primarily in the meristematic zone, hydrogen peroxide (H_2O_2) accumulates mainly in the differentiation zone^{5,6} and the balance between O_2^- and H_2O_2 modulates the transition from proliferation to differentiation⁶.

The RGF1 peptide is essential in controlling the size of the meristematic zone, acting as both an intrinsic and an extrinsic signal^{1,7,8}. Treating roots with RGF1 increases the size of the meristematic zone, and the *Arabidopsis rgf1/2/3* triple mutant has a smaller meristematic zone¹. Quintuple mutants of the *rgf1 receptor (rgfr)* lack most cells in the root meristem and are insensitive to RGF1 (refs. ^{2–4}). RGF1 signalling controls the stability of the PLETHORA (PLT) 1/2 proteins¹, which are required for stem cell maintenance⁹. However, it is not known how RGF1 modulates the size of the meristematic zone and the stability of PLT1/2.

We began by treating *Arabidopsis* roots with RGF1, and detected green fluorescent protein (GFP)-labelled HIGH PLOIDY2 (HPY2)¹⁰ (a marker protein specific to the meristematic zone) in an enlarged area that correlates with a larger meristematic zone (Extended Data Fig. 1a–c), suggesting that RGF1 controls gene expression primarily in this zone. Therefore, to identify target genes that are downstream of RGF1, we isolated the meristematic zone 1 h after RGF1 treatment (Extended Data Fig. 1d). Given that HPY2-GFP expression and the size of the meristematic zone were unchanged in this time period, we can exclude the possibility that an enlarged meristem is the reason for any changes in

RNA levels. RNA-sequencing (RNA-seq) profiling found 583 genes that were differentially expressed between the RGF1-treatment and mock-treatment scenarios (Supplementary Table 1). Gene Ontology highly enriched categories included 'glutathione transferase activity' and 'oxidoreductase activity' (Extended Data Fig. 2 and Supplementary Table 2), suggesting that RGF1 might signal through an ROS intermediate.

To examine the relationship between RGF1 and ROS signalling, we analysed the distribution of O_2^- and H_2O_2 after RGF1 treatment. A specific indicator for H_2O_2 —namely H_2O_2 -3'-O-acetyl-6'-O-pentafluorobenzenesulfonyl-2'-7'-difluorofluorescein-Ac (H_2O_2 -BES-Ac)⁶—exhibited lower fluorescence in the meristematic and elongation zones 24 h after RGF1 treatment (Fig. 1a, c). We detected O_2^- signals by nitro blue tetrazolium (NBT) staining⁵ and observed these signals more broadly in the meristematic zone 24 h after RGF1 treatment (Fig. 1b, d). In the RGF1-receptor mutant *rgf1/2/3*, the meristematic zone of which is unchanged after RGF1 treatment (Fig. 1e), levels of H_2O_2 and O_2^- were comparable between mock and RGF1 treatments (Fig. 1e–h).

To identify downstream factors in the RGF1 and ROS signalling pathway, we combined our RGF1 transcriptome data with developmental-zone-specific transcriptome data¹¹. Among genes that are both meristematic-zone-specific and induced by RGF1, we identified *PLANT AT-RICH SEQUENCE AND ZINC-BINDING TRANSCRIPTION FACTOR (PLATZ) FAMILY PROTEIN* (AT2G12646), the expression of which increased approximately twofold after 1 h of RGF1 treatment (Fig. 2a). We named this gene *RGF1-INDUCIBLE TRANSCRIPTION FACTOR 1 (RITF1)*, and found that its expression occurs predominantly in the meristematic zone¹¹ (Fig. 2b). Quantitative reverse transcription with polymerase chain reaction (RT-PCR) showed that the abundance of the *RITF1* transcript increased approximately twofold in wild-type roots 1 h after RGF1 treatment, and was maintained at 6 h and 24 h (Fig. 2c). By contrast,

¹Department of Biology and Howard Hughes Medical Institute, Duke University, Durham, NC, USA. ²Agricultural Biotechnology Research Center, Academia Sinica, Taipei, Taiwan.

³Biotechnology Center in Southern Taiwan, Academia Sinica, Tainan, Taiwan. ⁴Present address: GlaxoSmithKline, Waltham, MA, USA. *e-mail: philip.benfey@duke.edu

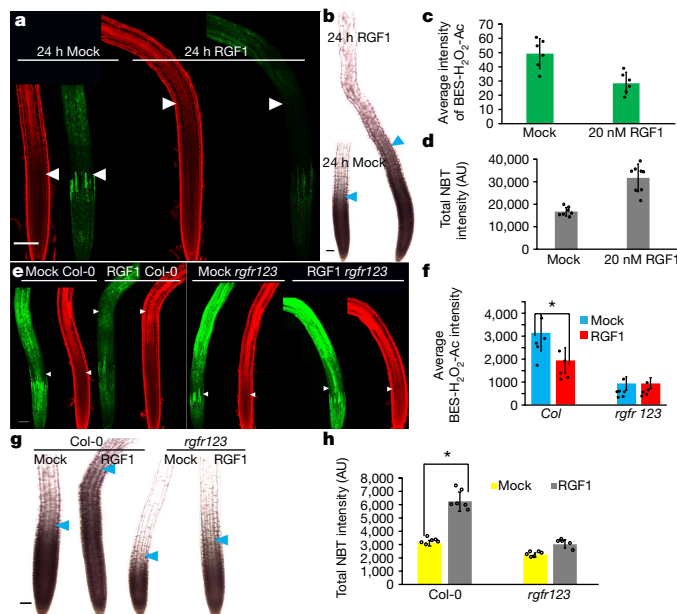


Fig. 1 | Distribution of ROS levels upon RGF1 treatment. **a**, Confocal images of roots 24 h after mock treatment or treatment with 20 nM RGF1. Propidium iodide (PI) staining is in red; H₂O₂-BES-Ac fluorescence is in green. **b**, Roots stained with NBT 24 h after mock treatment or treatment with 20 nM RGF1. **c**, Quantification of H₂O₂-BES-Ac intensity in the meristematic zone ($n=6$ independent roots; $P<0.003$). **d**, Quantification of NBT staining intensity (in arbitrary units, AU) in the meristematic zone ($n=7$ independent roots; $P=3.16 \times 10^{-5}$). **e**, Confocal images of roots 24 h after mock treatment or treatment with 20 nM RGF1 in wild-type roots (Columbia-0 (Col-0) background) or rgfr1/2/3 mutants. Staining as in **a**. **f**, Quantification of H₂O₂-BES-Ac staining intensity in the meristematic zone in wild-type and rgfr1/2/3 roots ($n=5$ independent roots; * $P<0.025$). **g**, Wild-type or rgfr1/2/3 roots stained with NBT 24 h after mock treatment or treatment with 20 nM RGF1. **h**, Quantification of NBT staining intensity in the meristematic zone of wild-type or rgfr1/2/3 roots ($n=5$ independent roots; * $P=1.65 \times 10^{-6}$). White and blue arrowheads indicate the junction between the meristematic and elongation zones. Scale bar, 50 μ m. Bar graphs show means. Error bars show \pm s.d. Dots indicate each data point. P values are calculated by two-sided Student's t-test.

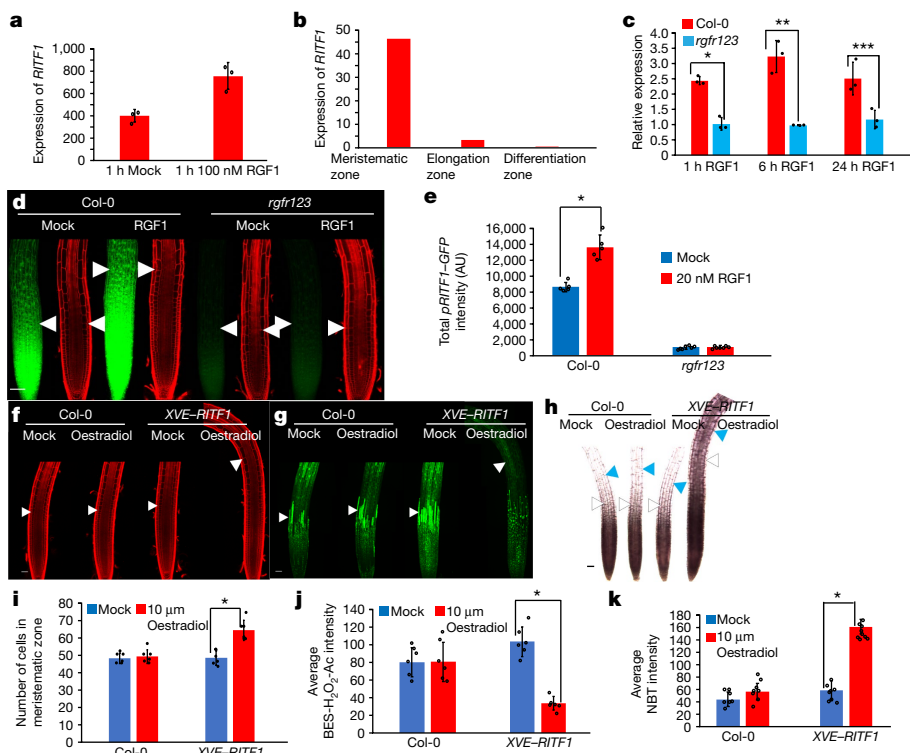


Fig. 2 | Expression of RITF1 and phenotype of RITF1 overexpression line.

a, Expression of RITF1 in the meristematic zone 1 h after treatment with 100 nM RGF1, measured by RNA-seq (CPM, counts per million mapped reads; $n=3$ independent experiments; $P<0.01$). **b**, Expression of RITF1 in developmental zones as measured by RNA-seq (FPKM, fragments per kilobase of transcript per million mapped reads). **c**, Expression of RITF1 in the meristematic zone of wild-type and rgfr1/2/3 roots upon treatment with RGF1, measured by quantitative RT-PCR ($n=3$ independent experiments; * $P<0.001$, ** $P<0.002$, *** $P<0.02$). **d**, Confocal images of pRITF1-GFP expression and PI staining in wild-type and rgfr1/2/3 roots after RGF1 treatment. **e**, Total intensity of pRITF1-GFP expression in wild-type and rgfr1/2/3 roots 24 h after RGF1 treatment ($n=5$ independent roots; * $P<0.001$). **f**, **g**, Confocal images of roots stained with PI (f) and NBT (g) 24 h after mock or oestradiol treatment. **h**, Light microscope images of NBT-stained roots after mock or oestradiol treatment. **i**, Number of cells in the meristematic zone in Col-0 and XVE-RITF1 roots after mock or oestradiol treatment ($n=6$ independent roots; * $P<0.001$). **j**, Average intensity of BES-H₂O₂-Ac in the differentiation zone after mock or oestradiol treatment ($n=6$ independent roots; * $P<0.001$). **k**, Average intensity of NBT staining in the differentiation zone after mock or oestradiol treatment ($n=7$ independent roots; * $P<0.001$). Scale bar, 50 μ m. White and blue arrowheads throughout indicate the junctions between the meristematic and elongation zones and between the elongation and differentiation zones. Bar graphs show means. Error bars are \pm s.d. Dots indicate each data point. P values are calculated by two-sided Student's t-test.

and H₂O₂-BES-Ac (g) in Col-0 and XVE-RITF1 roots after mock or oestradiol treatment. **h**, Light microscope images of NBT-stained roots after mock or oestradiol treatment. **i**, Number of cells in the meristematic zone in Col-0 and XVE-RITF1 roots after mock or oestradiol treatment ($n=6$ independent roots; * $P<0.001$). **j**, Average intensity of BES-H₂O₂-Ac in the differentiation zone after mock or oestradiol treatment ($n=6$ independent roots; * $P<0.001$). **k**, Average intensity of NBT staining in the differentiation zone after mock or oestradiol treatment ($n=7$ independent roots; * $P<0.001$). Scale bar, 50 μ m. White and blue arrowheads throughout indicate the junctions between the meristematic and elongation zones and between the elongation and differentiation zones. Bar graphs show means. Error bars are \pm s.d. Dots indicate each data point. P values are calculated by two-sided Student's t-test.

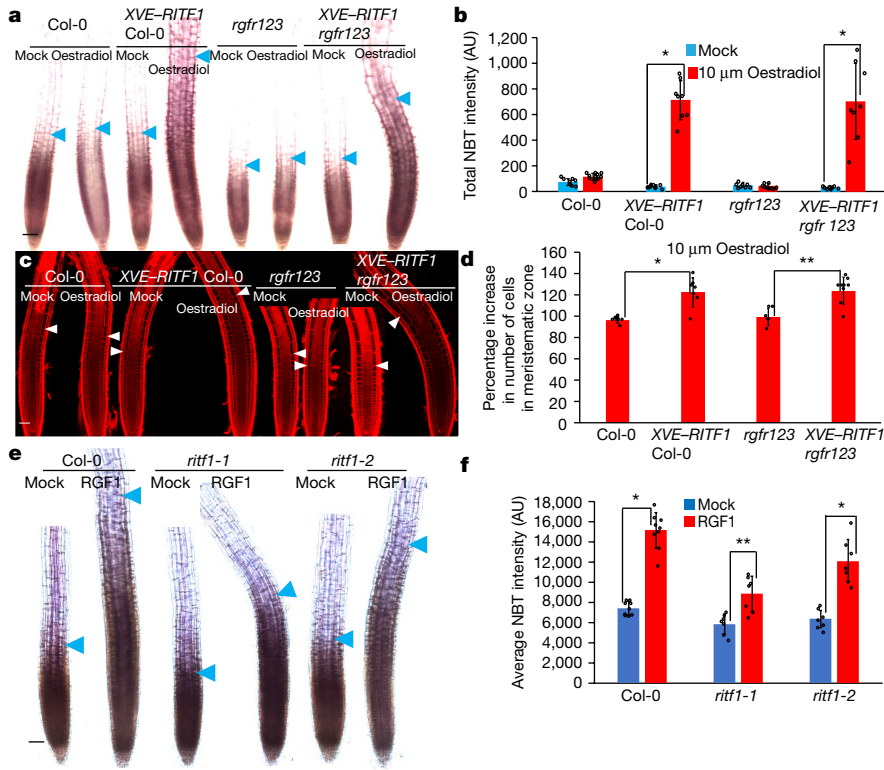


Fig. 3 | ROS signals and meristem size in RITF1 overexpression lines in rgfr1/2/3 roots. **a**, Light microscope images of NBT-stained roots with or without XVE-RITF1 expression in Col-0 and rgfr1/2/3 roots. **b**, Total intensity of NBT staining in the differentiation zone with or without XVE-RITF1 expression, in Col-0 and rgfr1/2/3 roots, 24 h after mock or oestradiol treatment ($n=8$ independent roots; $*P<2.0\times 10^{-5}$). **c**, Confocal images of PI-stained roots with or without XVE-RITF1 expression in Col-0 and rgfr1/2/3 roots. **d**, Percentage increase in the number of cells in the meristematic zone (in which 100% is the number of cells in the mock treatment scenario) 24 h after oestradiol treatment compared with mock treatment in Col-0 roots, rgfr1/2/3 roots, and XVE-RITF1-

expressing Col-0 and rgfr1/2/3 roots ($n=6$ independent roots; $*P<0.0002$, $**P<0.0007$). **e**, Light microscope images of roots of Col-0, rgfr1-1 and rgfr1-2 roots stained with NBT 24 h after 5 nM RGF1 treatment. Scale bar, 50 μm . Blue arrowheads show the junction between the meristematic and elongation zones. **f**, Quantification of NBT staining intensity in the meristematic zone in Col-0, rgfr1-1 and rgfr1-2 roots after 5 nM RGF1 treatment ($n=7$ independent roots; $*P\le 2.4\times 10^{-5}$, $**P<0.021$). Bar graphs show means. Error bars represent $\pm \text{s.d.}$ Dots indicate each data point. P values are calculated by two-sided Student's t -test.

RITF1 expression in rgfr1/2/3 roots was unchanged upon RGF1 treatment (Fig. 2c). Expression of a construct with the RITF1 promoter driving the GFP-coding sequence (*pRITF1-GFP*) mirrored our transcriptome analysis and increased in the wild type following RGF1 treatment (Fig. 2b, d, e). By contrast, *pRITF1-GFP* expression was very low and exhibited no change following RGF1 treatment in rgfr1/2/3 mutants (Fig. 2d, e). These data indicate that RITF1 expression is regulated by the RGF1 pathway.

To understand its function, we inducibly overexpressed RITF1 using the oestradiol-inducible promoter system^{12,13}. After 24 h of β -oestradiol treatment, the meristematic zone became enlarged and the number of cells increased (Fig. 2f, i), similarly to RGF1-treated roots (Fig. 1a). We also found that H_2O_2 levels declined in all three developmental zones upon oestradiol treatment (Fig. 2g, j), and that enhanced O_2^- signals were observed in a broader area of the meristematic zone (Fig. 2h, k), with ectopic O_2^- signals in the elongation and differentiation zones (Fig. 2h). Altered ROS signals and an enlarged meristem suggest that RITF1 can modulate ROS signalling and root meristem size downstream of the RGF1 pathway. We also observed an earlier response to the induction of RITF1 than to RGF1 treatment. A decrease in the H_2O_2 -BES-Ac signal was detected 4 h after oestradiol treatment (Extended Data Fig. 3a, b), in contrast to the lack of detectable change seen 4 h after RGF1 treatment in either the uninduced line or in the wild type (Extended Data Fig. 3a, b). Changes in ROS signals were first observed at approximately 6 h after RGF1 treatment in those lines (Extended Data Figs. 4i, j, o, p and 5b, c).

If RITF1 functions downstream of the RGF1-receptor pathway, then overexpression of RITF1 in rgfr1/2/3 mutants should rescue root

meristem defects and increase root meristem size. To test this hypothesis, we inducibly overexpressed RITF1 in rgfr1/2/3 mutants and in the wild type, and observed an enhanced O_2^- signal and increased root meristem size in both (Fig. 3a–d). Finally, we examined two *ritf1* mutant alleles. We generated the *ritf1-1* allele using CRISPR–Cas9; it contains a frameshift mutation early in the coding sequence, rendering it unlikely to produce a functional RITF1 protein. The *ritf1-2* allele has a transfer-DNA insertion in the intron, but still shows low expression of full-length *RITF1* and is likely to produce low levels of a functional protein. The *ritf1-1* mutant had a smaller meristem and lower root growth rate (Extended Data Fig. 6a, b) and was more resistant to RGF1 treatment than were wild-type plants or those with the weak allele, *ritf1-2* (Extended Data Fig. 6b, c). Further, there was lower induction of the O_2^- signal in *ritf1-1* mutants after RGF1 treatment than in the wild-type or *ritf1-2* background (Fig. 3e, f). Taken together, these results strongly suggest that RITF1 is a primary regulator of ROS signalling and root meristem size in the RGF1 signalling pathway.

To confirm post-translational regulation of PLT2, we compared transcriptional (*pPLT2-CFP*)¹⁴ and translational (*gPLT2-YFP*)¹⁴ fusion lines (in which CFP and YFP are cyan and yellow fluorescent protein, respectively). At 24 h after RGF1 treatment, we observed broader localization of *gPLT2-YFP* (Extended Data Fig. 7b), and the localization and expression of *pPLT2-CFP* were comparable between mock and RGF1 treatments—even though RGF1-treated roots had a larger meristematic zone (Extended Data Fig. 7a). The *gPLT2-YFP* signal decreased more gradually and was broadly localized in the larger meristematic zone after RGF1 treatment (Extended Data Fig. 7a–c). These results confirm that RGF1 regulates PLT2 post-translationally.

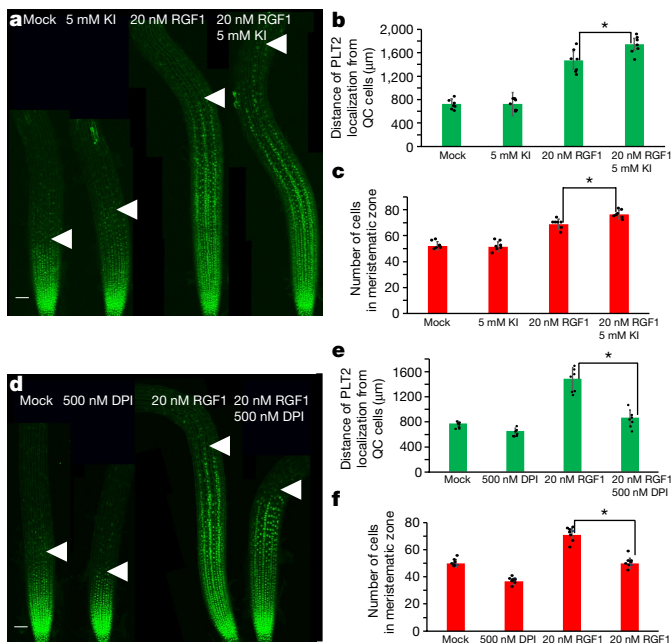


Fig. 4 | Stability of the PLT2 protein upon changes in oxidation conditions. **a, d**, Confocal images of gPLT2-YFP 24 h after treatment with RGF1, KI (a H₂O₂ scavenger) and DPI (an inhibitor of NADPH oxidase). **b, e**, Localization of gPLT2-YFP upon treatment with RGF1 and KI ($n=7$ independent roots; $*P<0.015$) and RGF1 and DPI ($n=7$ independent roots; $*P<1.5\times 10^{-5}$). **c, f**, Meristem size upon treatment with RGF1 and KI ($n=7$ independent roots, $*P<0.0017$) and RGF1 and DPI ($n=7$ independent roots, $*P<2.6\times 10^{-7}$). Bar graphs show means. Error bars show \pm s.d. Dots indicate each data point. Pvalues are calculated by two-sided Student's t-test. QC, quiescent centre.

PLT2 is a member of the APETALA2/ETHYLENE-RESPONSE FACTOR family of transcription factors, which has previously been reported to be regulated by oxidative post-translational modification^{15–20}. To determine whether modifying the oxidative conditions can increase the stability of the PLT2 protein, we treated the gPLT2-YFP line with RGF1 and potassium iodide (KI), an H₂O₂ scavenger. We found that gPLT2-YFP was localized more broadly and that meristem size was larger than in roots treated only with RGF1 (Fig. 4a–c). By contrast, increased H₂O₂ levels inhibited the broad localization of gPLT2-YFP and reduced the increase in meristem size upon addition of RGF1 (Extended Data Fig. 8a–e). To decrease O₂[−] levels, we used a low concentration (500 nM) of diphenyleneiodonium (DPI), an NADPH oxidase inhibitor (Fig. 4d–f), resulting in a slight inhibition of PLT2 stability and slight decrease in meristem size (Fig. 4d–f) with little effect on root meristem development. However, co-treatment using RGF1 and DPI markedly reduced PLT2 stability and meristem size as compared with RGF1 treatment alone (Fig. 4d–f). Finally, we measured gPLT2-YFP, O₂[−] and H₂O₂ levels in a time course (4–10 h) after RGF1 treatment. Broader localization of gPLT2-YFP and increased superoxide levels along with lower H₂O₂ signals at the distal end of the meristematic zone appeared 6 h after treatment (Extended Data Figs. 4a–d, i, j, o, p and 5a–c). At 8 h and 10 h after treatment, expanded gPLT2-YFP expression and O₂[−] signals correlated with declining H₂O₂ signals (Extended Data Figs. 4e–h, k–n, q–t and 5a–c). Taken together, these results indicate that ROS regulates PLT2 protein stability by modulating O₂[−] and H₂O₂ levels.

To further test the hypothesis that the stability of the PLT2 protein is enhanced by ROS signalling produced by RITF1, we overexpressed RITF1 in the plt2 mutant. This produced an increase in the O₂[−] signal (Extended Data Fig. 9a, b) but was unable to induce an increase in root meristem size (Extended Data Fig. 9c, d). Furthermore, we detected only a subtle change in root meristem size in plt2 mutants as compared with wild-type roots upon RGF1 treatment (Extended Data Fig. 10a, b).

However, we did observe an elevated O₂[−] signal (Extended Data Fig. 10c, d). These results strongly suggest that ROS signals modulated by RITF1 enhance PLT2 stability. In summary, we have identified a new transcription factor, RITF1, which is induced by RGF1 in the meristematic zone. This factor controls ROS levels, which in turn regulate PLT2 stability and meristem size. Overall, our data demonstrate a key role for the peptide hormone RGF1 in regulating root growth via modulation of ROS levels, which control the transition from proliferation to differentiation.

Online content

Any methods, additional references, Nature Research reporting summaries, source data, extended data, supplementary information, acknowledgements, peer review information; details of author contributions and competing interests; and statements of data and code availability are available at <https://doi.org/10.1038/s41586-019-1819-6>.

- Matsuzaki, Y., Ogawa-Ohnishi, M., Mori, A. & Matsubayashi, Y. Secreted peptide signals required for maintenance of root stem cell niche in *Arabidopsis*. *Science* **329**, 1065–1067 (2010).
- Ou, Y. et al. RGF1 INSENSITIVE 1 to 5, a group of LRR receptor-like kinases, are essential for the perception of root meristem growth factor 1 in *Arabidopsis thaliana*. *Cell Res.* **26**, 686–698 (2016).
- Song, W. et al. Signature motif-guided identification of receptors for peptide hormones essential for root meristem growth. *Cell Res.* **26**, 674–685 (2016).
- Shinohara, H., Mori, A., Yasue, N., Sumida, K. & Matsubayashi, Y. Identification of three LRR-RKs involved in perception of root meristem growth factor in *Arabidopsis*. *Proc. Natl Acad. Sci. USA* **113**, 3897–3902 (2016).
- Dunand, C., Crévecoeur, M. & Penel, C. Distribution of superoxide and hydrogen peroxide in *Arabidopsis* root and their influence on root development: possible interaction with peroxidases. *New Phytol.* **174**, 332–341 (2007).
- Tsukagoshi, H., Busch, W. & Benfey, P. N. Transcriptional regulation of ROS controls transition from proliferation to differentiation in the root. *Cell* **143**, 606–616 (2010).
- Whitford, R. et al. GOLVEN secretory peptides regulate auxin carrier turnover during plant gravitropic responses. *Dev. Cell* **22**, 678–685 (2012).
- Meng, L., Buchanan, B. B., Feldman, L. J. & Luan, S. CLE-like (CLEL) peptides control the pattern of root growth and lateral root development in *Arabidopsis*. *Proc. Natl Acad. Sci. USA* **109**, 1760–1765 (2012).
- Aida, M. et al. The PLETHORA genes mediate patterning of the *Arabidopsis* root stem cell niche. *Cell* **119**, 109–120 (2004).
- Ishida, T. et al. SUMO E3 ligase HIGH PLOIDY2 regulates endocycle onset and meristem maintenance in *Arabidopsis*. *Plant Cell* **21**, 2284–2297 (2009).
- Li, S., Yamada, M., Han, X., Ohler, U. & Benfey, P. N. High-resolution expression map of the *Arabidopsis* root reveals alternative splicing and lincRNA regulation. *Dev. Cell* **39**, 508–522 (2016).
- Curtis, M. D. & Grossniklaus, U. A gateway cloning vector set for high-throughput functional analysis of genes in planta. *Plant Physiol.* **133**, 462–469 (2003).
- Zuo, J., Niu, Q. W. & Chua, N. H. Technical advance: an estrogen receptor-based transactivator XVE mediates highly inducible gene expression in transgenic plants. *Plant J.* **24**, 265–273 (2000).
- Galinha, C. et al. PLETHORA proteins as dose-dependent master regulators of *Arabidopsis* root development. *Nature* **449**, 1053–1057 (2007).
- Waszczak, C. et al. Sulphenome mining in *Arabidopsis thaliana*. *Proc. Natl Acad. Sci. USA* **111**, 11545–11550 (2014).
- Licausi, F., Ohme-Takagi, M. & Perata, P. APETALA2/ethylene responsive factor (AP2/ERF) transcription factors: mediators of stress responses and developmental programs. *New Phytol.* **199**, 639–649 (2013).
- Shaikhali, J. et al. The redox-sensitive transcription factor Rap2.4a controls nuclear expression of 2-Cys peroxiredoxin A and other chloroplast antioxidant enzymes. *BMC Plant Biol.* **8**, 48 (2008).
- Dietz, K. J., Vogel, M. O. & Viehhauser, A. AP2/EREBP transcription factors are part of gene regulatory networks and integrate metabolic, hormonal and environmental signals in stress acclimation and retrograde signalling. *Protoplasma* **245**, 3–14 (2010).
- Licausi, F. et al. Oxygen sensing in plants is mediated by an N-end rule pathway for protein destabilization. *Nature* **479**, 419–422 (2011).
- Welsch, R., Maass, D., Voegel, T., Dellapenna, D. & Beyer, P. Transcription factor RAP2.2 and its interacting partner SINAT2: stable elements in the carotenogenesis of *Arabidopsis* leaves. *Plant Physiol.* **145**, 1073–1085 (2007).
- Wang, Z. P. et al. Egg cell-specific promoter-controlled CRISPR/Cas9 efficiently generates homozygous mutants for multiple target genes in *Arabidopsis* in a single generation. *Genome Biol.* **16**, 144 (2015).
- Maeda, H. et al. Fluorescent probes for hydrogen peroxide based on a non-oxidative mechanism. *Angew. Chem. Int. Edn* **43**, 2389–2391 (2004).
- Schindelin, J. et al. Fiji: an open-source platform for biological-image analysis. *Nat. Methods* **9**, 676–682 (2012).

Publisher's note Springer Nature remains neutral with regard to jurisdictional claims in published maps and institutional affiliations.

Methods

Plant materials and growth conditions

All *Arabidopsis* mutants and marker lines used here are in the Columbia-0 (Col-0) background. The transfer (T)-DNA *plt2* insertion line (SALK_130119.20.25) was obtained from the *Arabidopsis* Biological Resource Center at Ohio State University. The T-DNA insertion was found to be 166 base pairs upstream of the transcription start site in the *plt2* mutant. Seeds were surface-sterilized using 50% (v/v) bleach and 0.1% Tween 20 (Sigma) for 15 min and then rinsed five times with sterile water. All seeds were plated on standard MS medium (1 × Murashige and Skoog salt mixture, Caisson Laboratories), 0.5 g l⁻¹ MES, 1% sucrose and 1% agar (Difco) and adjusted to pH 5.7 with KOH. All plated seeds were stratified at 4 °C for 2 days before germination. Seedlings were grown on vertically positioned square plates in a Percival incubator with 16 h of daily illumination at 22 °C.

The *ritf1* mutants

The *ritf1-1* mutant was generated using the egg-cell-specific controlled CRISPR–Cas9 system²¹.

sgRNA sequences are as follows: *RITF1* sgRNA1, GGGATGTCCA TACCATGAGA CGG; *RITF1* sgRNA2, CCGTCTACCACAGTTGATCG AGG; *RITF1* sgRNA3, GGCAGACTTGAAGGAGTCA TGG; and *RITF1* sgRNA4, GACTTCAGTTGAGTCCTCA TGG.

The CRISPR construct was transformed into the Col-0 background using the *Agrobacterium*-mediated floral dip method. The mutant was identified by direct sequencing of PCR products of the targets in the offspring in T1, T2 and T3 generations. The loss-of-function *ritf1-1* allele contains an insertion of a cytosine 74 bp after the transcription start site in the *RITF1* gene (771 bp). The additional insertion of a cytosine results in a frameshift and creates many premature stop codons after the insertion. To exclude issues related to off-target mutations, we confirmed the sequences of three potential off-target genes (At5g25170, At1g70110 and At3g20640) that include similar sequences of the target sites by direct sequencing of PCR products in the offspring in the T1, T2 and T3 generations. We did not find any mutations in these genes. Further, we identified another independent CRISPR allele (*ritf1-3*). This allele contains an insertion of an adenine 75 bp after the transcription start site in the *RITF1* gene. The additional insertion of an adenine results in a frameshift and creates many premature stop codons after the insertion. Similar to *ritf1-1* mutants, *ritf1-3* seedlings exhibited strong resistance to the RGF1 peptide and did not increase their O₂⁻ levels by comparison with wild-type seedlings or with the weak allele (*ritf1-2*) (Extended Data Fig. 6d, e). These results exclude the possibility that off-target mutations cause the RGF1-resistant phenotype.

In the *ritf1-2* allele (SALK_081503C), we identified the T-DNA insertion 787 bp downstream of the transcription start site (in the middle of the second intron) of *RITF1*. Even though the insertion disrupted an intron, a full-length transcript was weakly detected from this allele.

Detecting *gPLT2-YFP* and ROS signals

We grew wild-type and *rgfr1/2/3* mutant plants for seven days on MS agar plates, then transferred them to MS agar plates containing either water (mock treatment) or 20 nM synthetic sulfated RGF1 peptide (Invitrogen). After treatment with RGF1, seedlings were stained for 2 min in a solution of 200 μM NBT in 20 mM phosphate buffer (pH 6.1) in the dark and rinsed twice with distilled water. To detect hydrogen peroxide with BES-H₂O₂-Ac²², we incubated seedlings in 50 μM BES-H₂O₂-Ac (WAKO) for 30 min in the dark, then mounted them in 10 mg ml⁻¹ PI in water⁶. Roots were observed using a ×20 objective with a Zeiss LSM 880 laser scanning confocal microscope. Excitation and detection windows were set as follows: BES-H₂O₂-Ac, excitation at 488 nm and detection at 500–550 nm; PI staining, excitation at 561 nm and detection at 570–650 nm. Confocal images were processed, stitched and analysed using the Fiji package of ImageJ²³. Maximum projection images were

generated from about 30 z-section images of BES-H₂O₂-Ac staining. The average intensity of BES-H₂O₂-Ac in the meristematic zone was measured in five or six roots with three biological replicates. Images for NBT staining were obtained using a ×10 objective with a Leica DM 5000-B light microscope. The total intensities of NBT staining in the meristematic zone were measured in ten roots with three biological replicates using the Fiji software package²³.

For experiments with a shorter time course, we grew *gPLT2-YFP* seedlings¹⁴ on MS agar plates for seven days, then transferred them to MS agar plates containing either water (mock) or 100 nM RGF1 peptide. At 4 h, 6 h, 8 h and 10 h after mock or RGF1 treatment, images were taken with a confocal or light microscope after PI, NBT and BES-H₂O₂-Ac staining, as above.

Total RNA extraction and library preparation

The *HYP2-GFP*¹⁰ line was grown on MS plates for seven days. *HYP2-GFP* seedlings were then transferred into liquid MS medium and treated with water (mock) or 100 nM RGF1 peptide in 6-well plates for 1 h. After mock or RGF1 treatment, the seedlings were taken out of liquid MS medium and transferred onto a 2% agarose plate. Using an ophthalmic scalpel (Feather), the meristematic zone of the seedlings was precisely dissected on the basis of *HYP2-GFP* fluorescence as detected under a dissecting microscope (Axio Zoom, Zeiss). Using the RNeasy Micro Kit (Qiagen), we extracted total RNA from 20 root sections treated with water (mock) or 100 nM RGF1. For each treatment, three replicates of the RNA extractions were performed. All total RNA samples were treated with DNase I during RNA extraction. RNA quality was examined using a 2100 Bioanalyzer (Agilent). The RNA integrity number was more than 9.0 in all samples. The concentration of total RNA was measured by a Qubit (Invitrogen) instrument. For each replicate, we generated complementary DNA (cDNA) from 50 ng total RNA using the Ovation RNA-seq System V2 (NuGEN). We fragmented 3 μg of the cDNA using the Covaris S-Series System. We used 400 ng of the fragmented cDNA with an average size of 400 bp for library preparation with the Ovation Ultralow System V2 (NuGEN). Illumina sequencing was performed at the Duke Genome Sequencing Shared Resource. The libraries for three biological replicates of mock- and RGF1-treated meristematic zones were sequenced on an Illumina HiSeq 2000 (100 base paired end reads).

Differential expression analysis after RGF1 treatment

Illumina sequencing reads were mapped to the TAIR10 *Arabidopsis* genome using Tophat V2.1.1. The parameters used for mapping were: ‘-N 5–read-gap-length 5–read-edit-dist 5–b2-sensitive -r 100–mate-std-dev 150 -p 5 -i 5 -I 15000 –min-segment-intron 5–max-segment-intron 15000–library-type fr-unstranded’. To select properly mapped reads with unique mapping positions, we kept for further analysis only those alignments with a flag of 83, 99, 147 or 163 and a mapping quality score of 50. Mapping positions of these reads were compared with the Araport11 genome annotation (https://www.araport.org/downloads/Araport11_Release_201606/annotation) using HTseq-count (v0.6.1) with parameters ‘-stranded=no–mode=intersection-nonempty’, which generated a read count per gene. The raw read counts of microRNAs, long non-coding RNAs and protein-coding genes were then used as input into DESeq2 (v1.14.1) for differential gene expression analysis. Genes with a false discovery rate (FDR)-adjusted *P* value less than or equal to 0.1 were regarded as differentially expressed between the RGF and mock treatment scenarios. The enriched Gene Ontology (GO) groups among differentially expressed genes were identified using agriGO. The GO annotation downloaded from <http://geneontology.org> was used as input for agriGO. Enriched GO groups required an FDR-adjusted *P* value of 0.01 or less and a minimum mapping entry of 10.

qRT-PCR analysis of *RITF1* expression upon RGF1 treatment

To perform qRT-PCR, we dissected about 20 meristematic zones of wild-type and *rgfr1/2/3* mutant roots at 1 h, 6 h and 24 h after RGF1 treatment

Article

as described above. We generated cDNA from 10 µg of total RNA using SuperScript IV Reverse Transcriptase (Invitrogen). Three biological replicates and technical replicates were used for each experiment. Standard curves were run for the primer pairs of: *RITF1*, 5'-CAAGCCAT-GCCACACTCTAA-3' and 5'-TTATCCGAGGAAGCTGAGGA-3'; and (as reference) *PROTEIN PHOSPHATASE 2A SUBUNIT A3* (*PP2AA3*, AT1G13320), 5'-GGCCAAAATGATGCAATCTC-3' and 5'-TGCAGAAATACCGAACAT-CAA-3'. Expression of *RITF1* was assayed by qRT-PCR on a LightCycler 480 (Roche) with SYBR-based detection, normalized to *PP2AA3*, and analysed by the efficiency-corrected quantification model.

Plasmid constructs

To produce the overexpression line and the transcriptional reporter line of *RITF1*, we amplified the coding sequence (771 bp) or the promoter sequence (2,121 bp) of the *RITF1* gene (AT2G12646) using the Phusion High-Fidelity DNA polymerase (New England Biolabs) from a wild-type cDNA library and genomic DNA, respectively, then subcloned into the pENTR/D/TOPO vector (Invitrogen). We used the following primers to amplify the coding sequence: 5'-CACCATGGGAATTTCAGAAACCGG-3' and 5'-TTAACAGAGAGGAGATCGTTG-3'; and for the promoter, 5'-CA CCGCATCTTTATTATAACCGA-3' and 5'-GAGGACTCACTGAA AGTCA-3'. We confirmed the sequences of the coding sequence and the promoter in the pENTR/D/TOPO vector using Sanger sequencing. The clones were recombined into the pMDC7 and pMDC204 vectors¹² using LR clonase II (Invitrogen) in order to fuse the oestradiol-inducible promoter (*XVE*)¹³ with the coding region of *RITF1*, the *RITF1* promoter and GFP with a carboxy-terminus HDEL retention sequence.

Meristem size and ROS detection after *RITF1* overexpression

We transformed the *XVE-RITF1* construct into the wild-type (Col-0) background. To measure meristem size and detect ROS signals, we grew two independent *XVE-RITF1* and wild-type lines on MS medium for seven days, then transferred them to MS medium containing dimethyl-sulfoxide (DMSO, mock) or 10 µM β-oestradiol (Sigma). After 24 h with mock or oestradiol treatment, we measured meristem size and detected ROS signals in the wild-type and *XVE-RITF1* lines, as above.

Expression of *pRITF1-GFP* in roots

We introduced the *pRITF1-GFP* construct into wild-type (Col-0) and *rgfr1/2/3* plants. We grew two independent T3 lines of each background for seven days in MS medium and treated them with either water (mock) or 20 nM RGF1 peptide. As described above, 24 h after treatment, GFP signals were detected using a confocal laser scanning microscope.

Note

UPB1 is not required for the RGF1-receptor pathway. It has previously been reported that UPBEAT1 (*UPB1*) reduces H₂O₂ levels and controls meristem size by downregulating peroxidase genes in the elongation zone⁶. However, our present transcriptome analysis did not find substantial changes in *UPB1* expression upon RGF1 treatment (Supplementary Tables 1, 3). We did find elevated expression

of five peroxidase genes (Supplementary Table 1), but these are not targets of *UPB1* (ref. ⁶), suggesting that RGF1 regulates meristem size independently of *UPB1*. To determine whether the peroxidase genes upregulated by RGF1 play a part in controlling meristem size in the RGF1-signalling pathway, we overexpressed two of them (At5g39580 and At4g08780). In neither case did we observe a larger meristematic zone (data not shown).

Statistics and reproducibility

Experiments were independently repeated three times with similar results. No power analysis was done to estimate sample size. The experiments were not randomized and investigators were not blinded to allocation during experiments and outcome assessment.

Reporting summary

Further information on research design is available in the Nature Research Reporting Summary linked to this paper.

Data availability

All RNA-seq data from this study have been deposited in the National Center for Biotechnology Information (NCBI) Gene Expression Omnibus (GEO), with the accession number GSE108730. Source data for all graphs have been provided. A previous version of this work was deposited in the preprint depository server bioRxiv at <https://doi.org/10.1101/244947>. Source Data for Figs. 1–4 and Extended Data Figs. 1, 3, 5–10 are provided with the paper. All other data are available from the corresponding author upon reasonable request.

Code availability

All code from this study is available upon request.

Acknowledgements We thank I. Taylor, J. Dickinson, E. Pierre-Jerome, K. Lehner and C. Winter for comments on the manuscript; C. Wilson for help with generating overexpression lines; G. Yang for help in identifying CRISPR mutants; K. Sugimoto for *HYP2-GFP* seeds; Y. Matsubayashi for *rgfr1/2/3* seeds; R. Heidstra for *gPLT2-YFP* and *pPLT2-CFP* seeds; N.-H. Chua for the pMDC7 vector; The Duke Genome Sequencing Center for sequencing Illumina libraries; the Plant Tech Core Facility in the Agricultural Biotechnology Research Center for generating the CRISPR construct; and the Transgenic Plant Laboratory at Academia Sinica for transforming the CRISPR construct into plants. This work was funded by the Howard Hughes Medical Institute and the Gordon and Betty Moore Foundation (through grant GBMF3405), the US National Institutes of Health (MIRA 1R35GM131725) to P.N.B., and Academia Sinica, Taiwan, to M.Y.

Author contributions M.Y. and P.N.B. conceptualized the study; M.Y. performed all experiments; X.H. performed the computational analyses; all authors wrote the paper.

Competing interests The authors declare no competing interests.

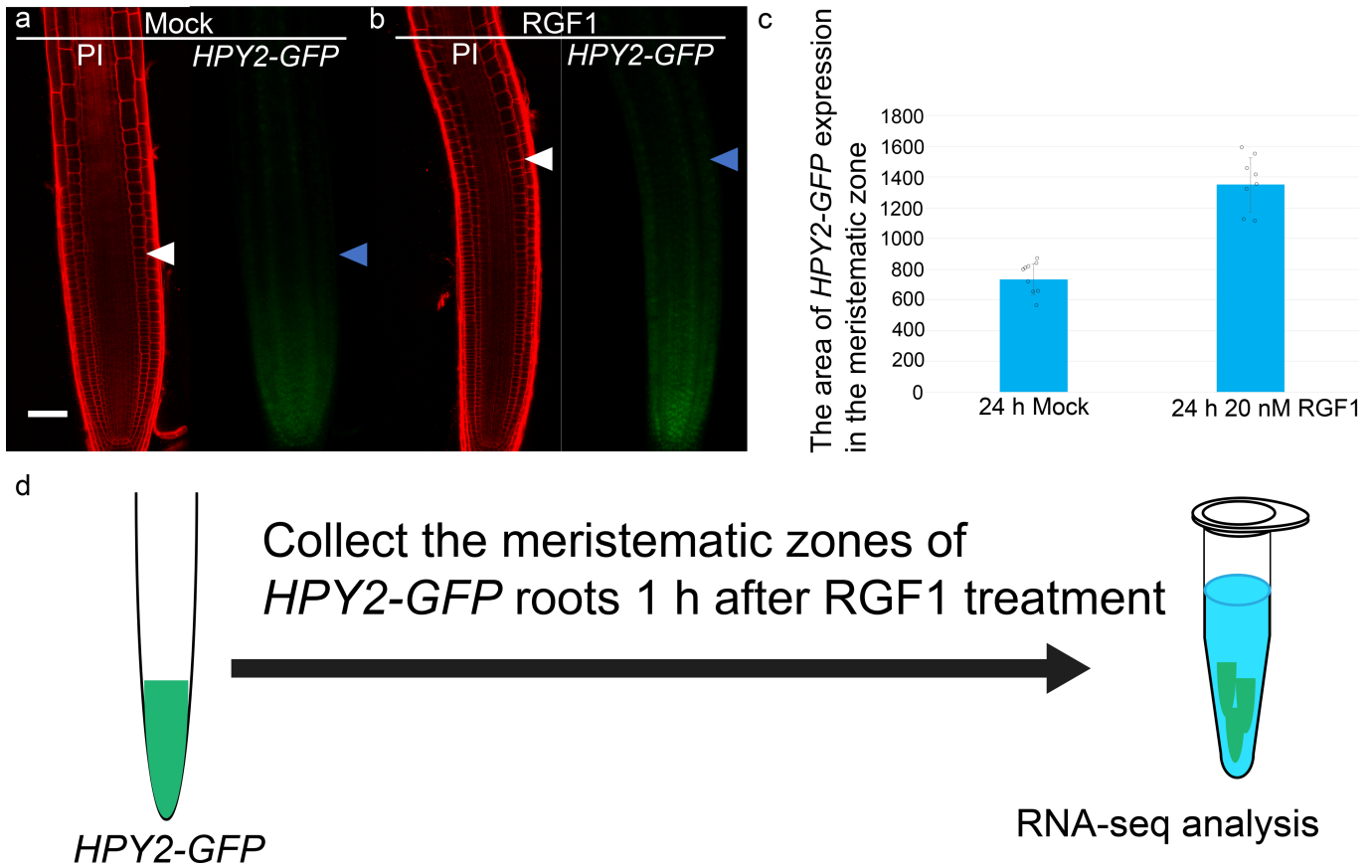
Additional information

Supplementary information is available for this paper at <https://doi.org/10.1038/s41586-019-1819-6>.

Correspondence and requests for materials should be addressed to P.N.B.

Peer review information *Nature* thanks Yoshikatsu Matsubayashi and the other, anonymous, reviewer(s) for their contribution to the peer review of this work.

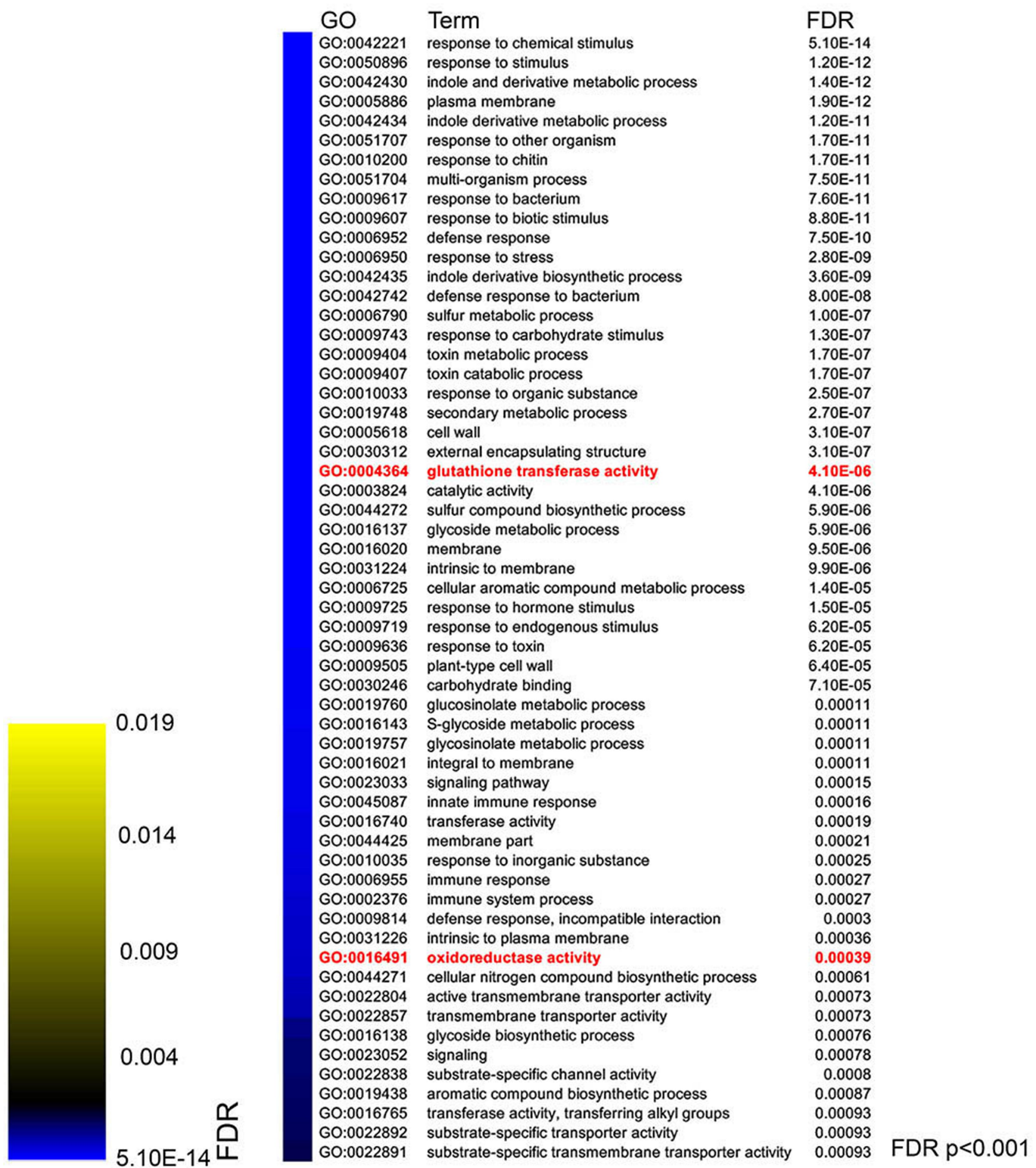
Reprints and permissions information is available at <http://www.nature.com/reprints>.



Extended Data Fig. 1 | Expression of meristematic-zone marker and transcriptome analysis upon RGF1 treatment. **a, b**, Confocal images of *HPY2-GFP* roots 24 h after treatment with water (mock; **a**) or 20 nM RGF1 (**b**). Seedlings were grown on MS plates for seven days before treatment. Left, PI-stained roots; right, GFP signals. White and blue arrowheads indicate the

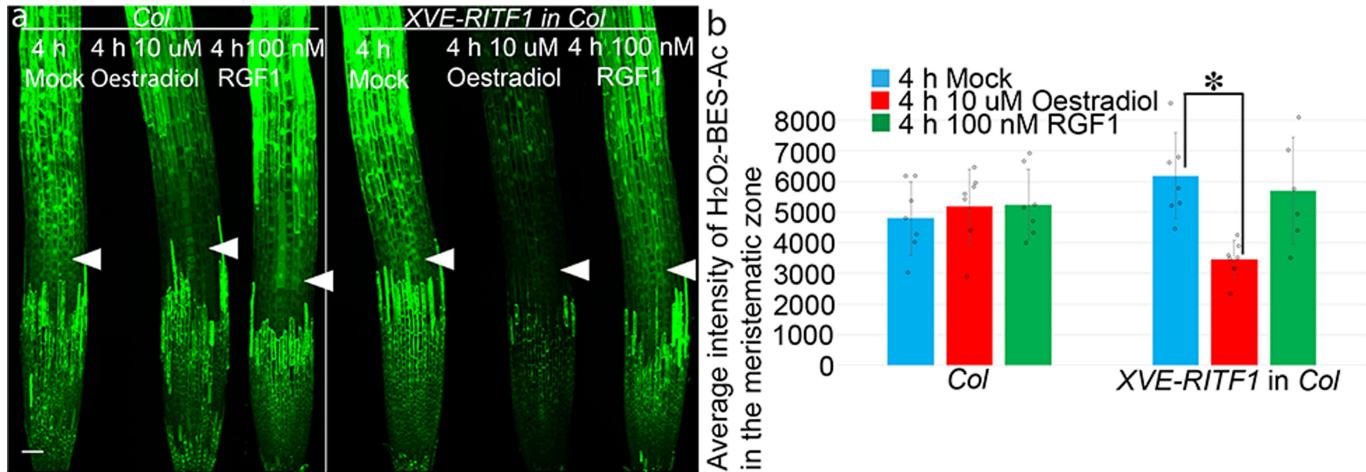
junction between the meristematic and elongation zones. Scale bar, 50 μm . **c**, Area of *HPY2-GFP* expression (in μm^2 ; $n = 8$ independent roots; $P < 2.1 \times 10^{-7}$). Bar graphs show means. Error bars are \pm s.d. Dots indicate each data point. *P* values are calculated by two-sided Student's *t*-test. **d**, Method of RNA extraction following RGF1 treatment.

Article



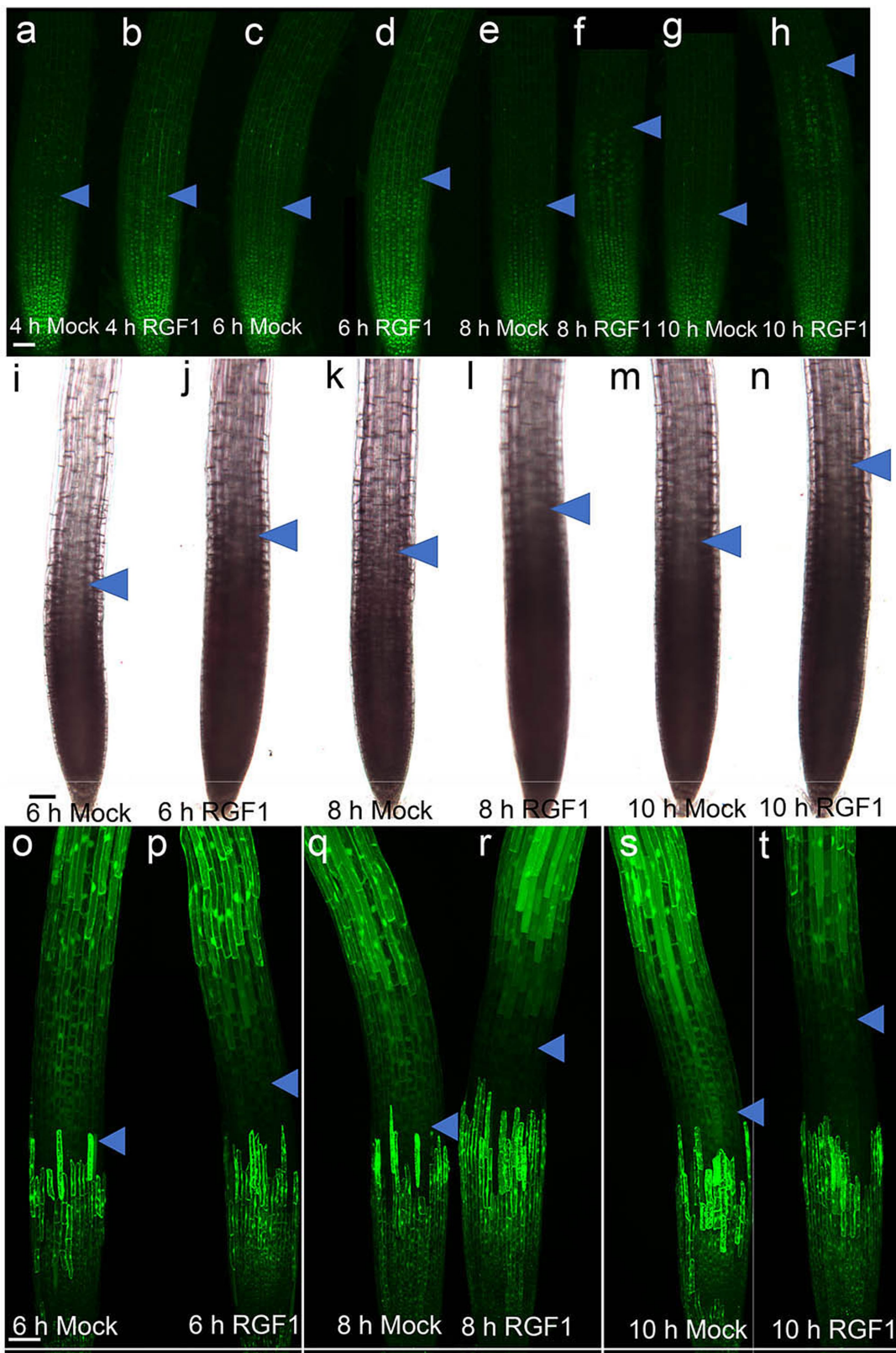
Extended Data Fig. 2 | GO categories that are enriched upon RGF1 treatment. These highly significantly enriched GO categories within lists of genes are regulated by RGF1 (FDR-adjusted $P < 0.001$), and include glutathione transferase activity (FDR-adjusted $P = 4.1 \times 10^{-6}$, red) and oxidoreductase

activity (FDR-adjusted $P = 0.00039$, red). See Supplementary Table 2 (enriched GO categories upon RGF1 treatment). P-values for GO enrichment analysis are based on Fisher's exact test, with the sample size being all genes in the genome and using a Benjamini–Yekutieli FDR for multiple testing correction.



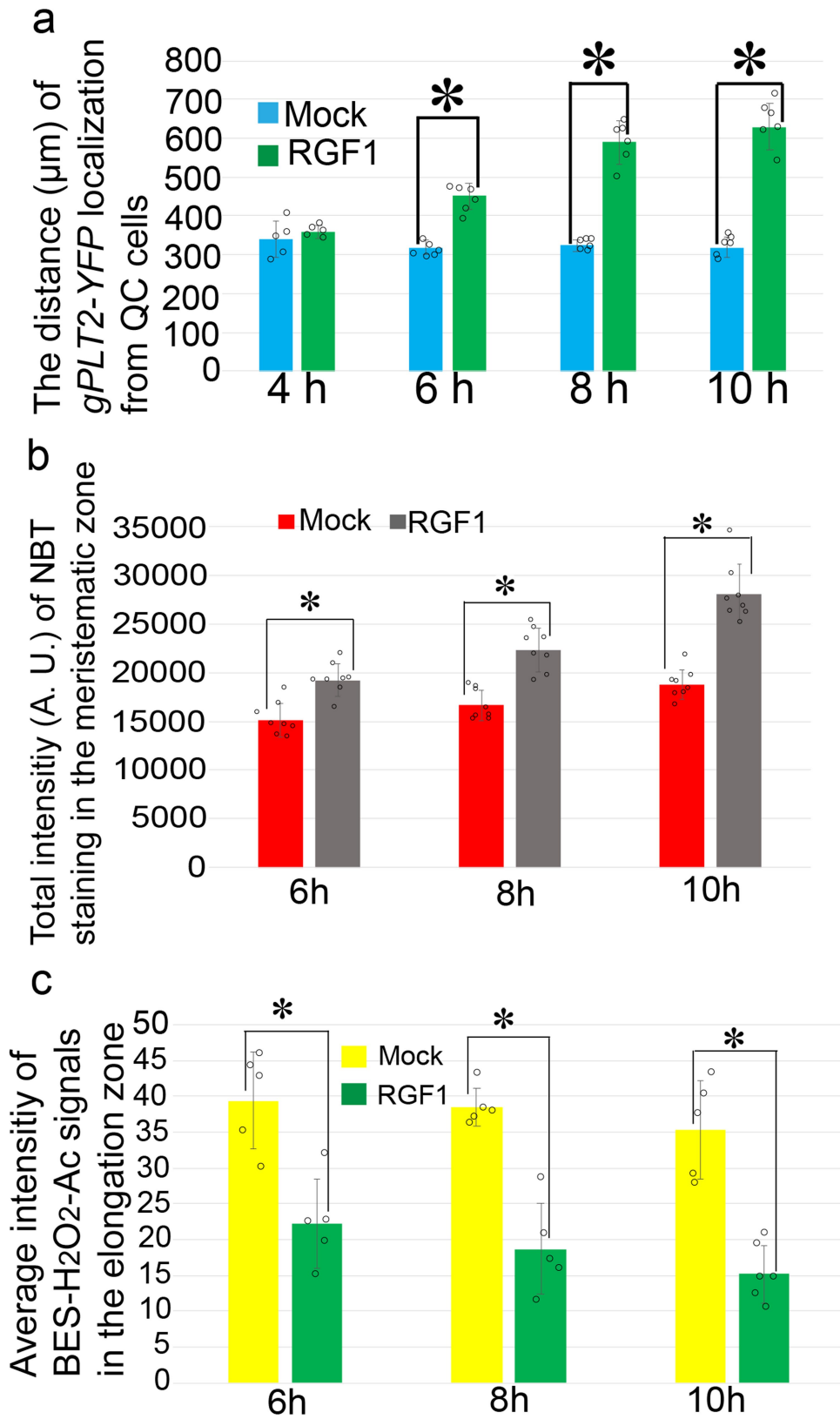
Extended Data Fig. 3 | H_2O_2 levels after inducible overexpression of *RITF1* and RGF1 treatment. a, Confocal images of $\text{H}_2\text{O}_2\text{-BES-Ac}$ stained roots, with or without *XVE-RITF1* expression, in a wild-type (*Col-0*) background 4 h after treatment with water (mock), 10 μM oestradiol or 100 nM RGF1.

b, Quantification of $\text{H}_2\text{O}_2\text{-BES-Ac}$ intensity in the meristematic zone ($n=6$ independent samples; $*P < 0.0005$). Bar graphs show means. Error bars are $\pm \text{s.d.}$. Dots indicate each data point. P values are calculated by two-sided Student's *t*-test.



Extended Data Fig. 4 | Localization of gPLT2-YFP, NBT and H_2O_2 -BES-Ac staining after RGF1 treatment. **a–t,** Localization of gPLT2-YFP (a–h), NBT staining (i–n) and H_2O_2 -BES-Ac staining (o–t), 4 h after treatment with water (mock; a) or 100 nM RGF1 (b), 6 h after treatment with water (mock; c, i, o) or 100 nM RGF1 (d, j, p), 8 h after treatment with water (mock; e, k, q) or 100 nM

RGF1 (f, l, r), or 10 h after treatment with water (mock; g, m, s) or 100 nM RGF1 (h, n, t). Blue arrowheads indicate the junction between the meristematic and elongation zones. Scale bar, 50 μm . Seedlings were grown on MS agar plates for seven days before treatment. Experiments were independently repeated three times with similar results.



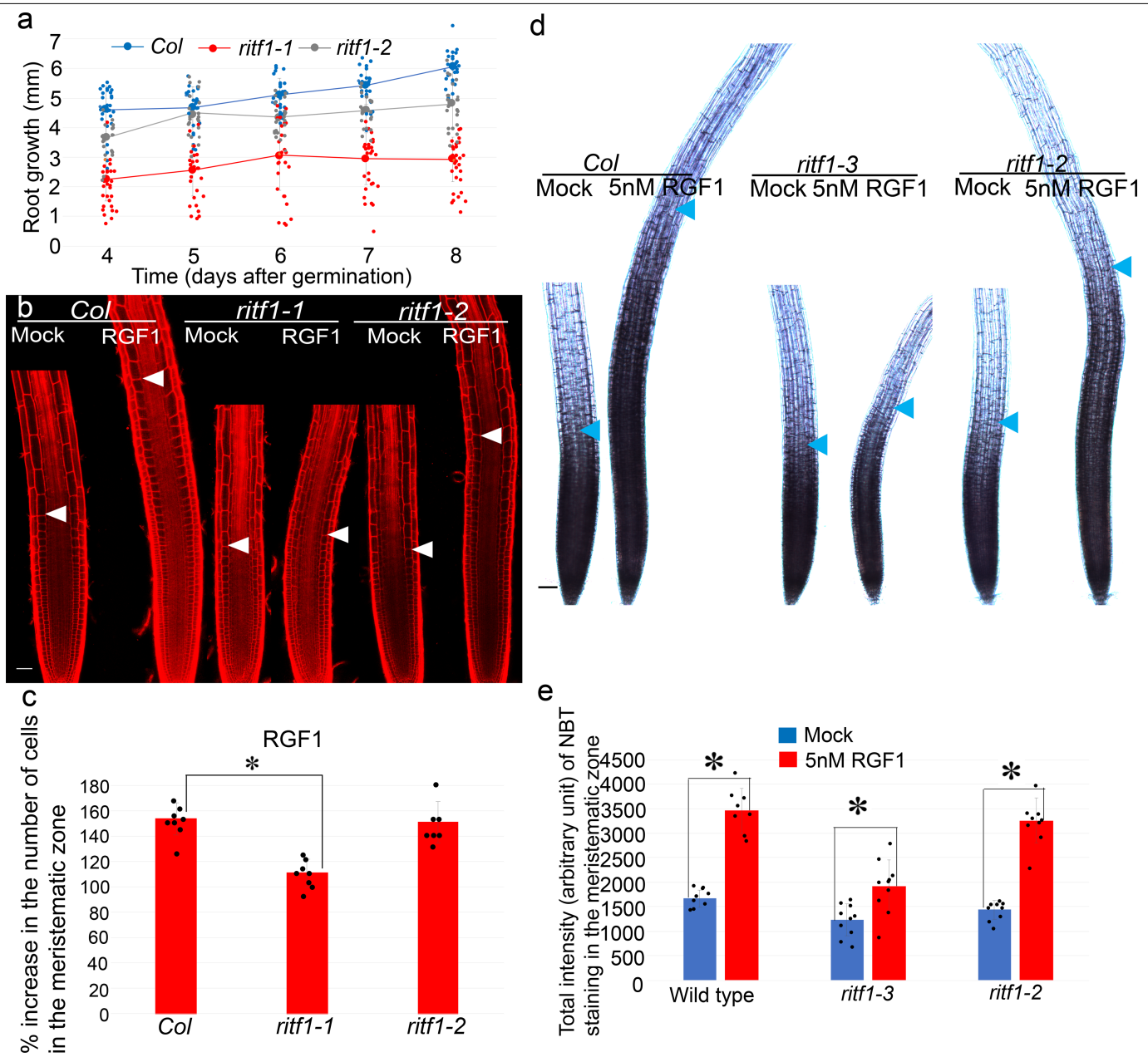
Extended Data Fig. 5 | Time course of gPLT2-YFP localization and NBT and H_2O_2 -BES-Ac staining. **a**, Distance (in μm) of gPLT2-YFP localization from

quiescent-centre cells ($n=5$ independent roots; $P<5.7\times 10^{-6}$). **b**, Total intensity of NBT staining in the meristematic zone ($n=8$ independent roots; $P<0.0003$).

c, Average intensity of H_2O_2 -BES-Ac staining in the elongation zone ($n=5$

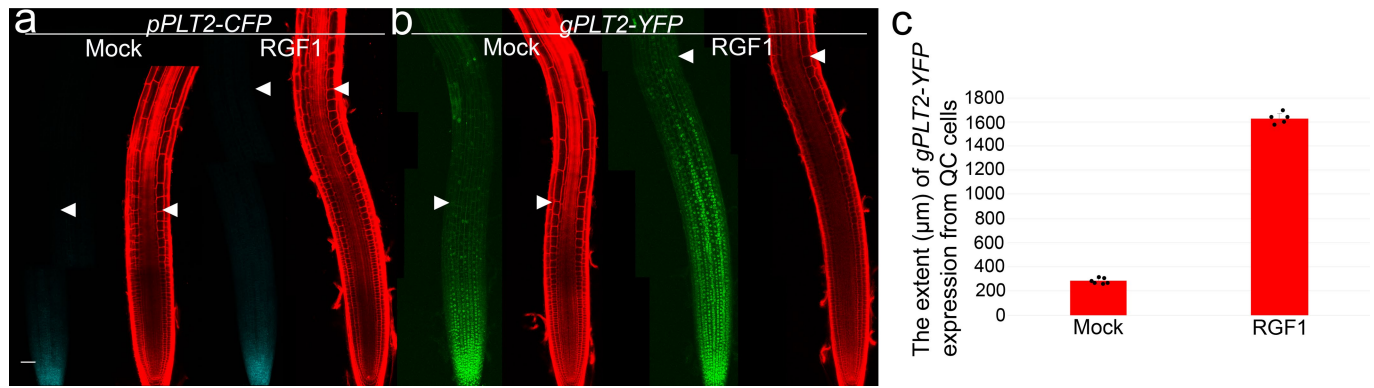
independent roots; $P<0.003$). Bar graphs show means. Error bars are $\pm \text{s.d.}$. Dots indicate each data point. Pvalues are calculated by two-sided Student's *t*-test. Experiments were independently repeated three times with similar results.

Article



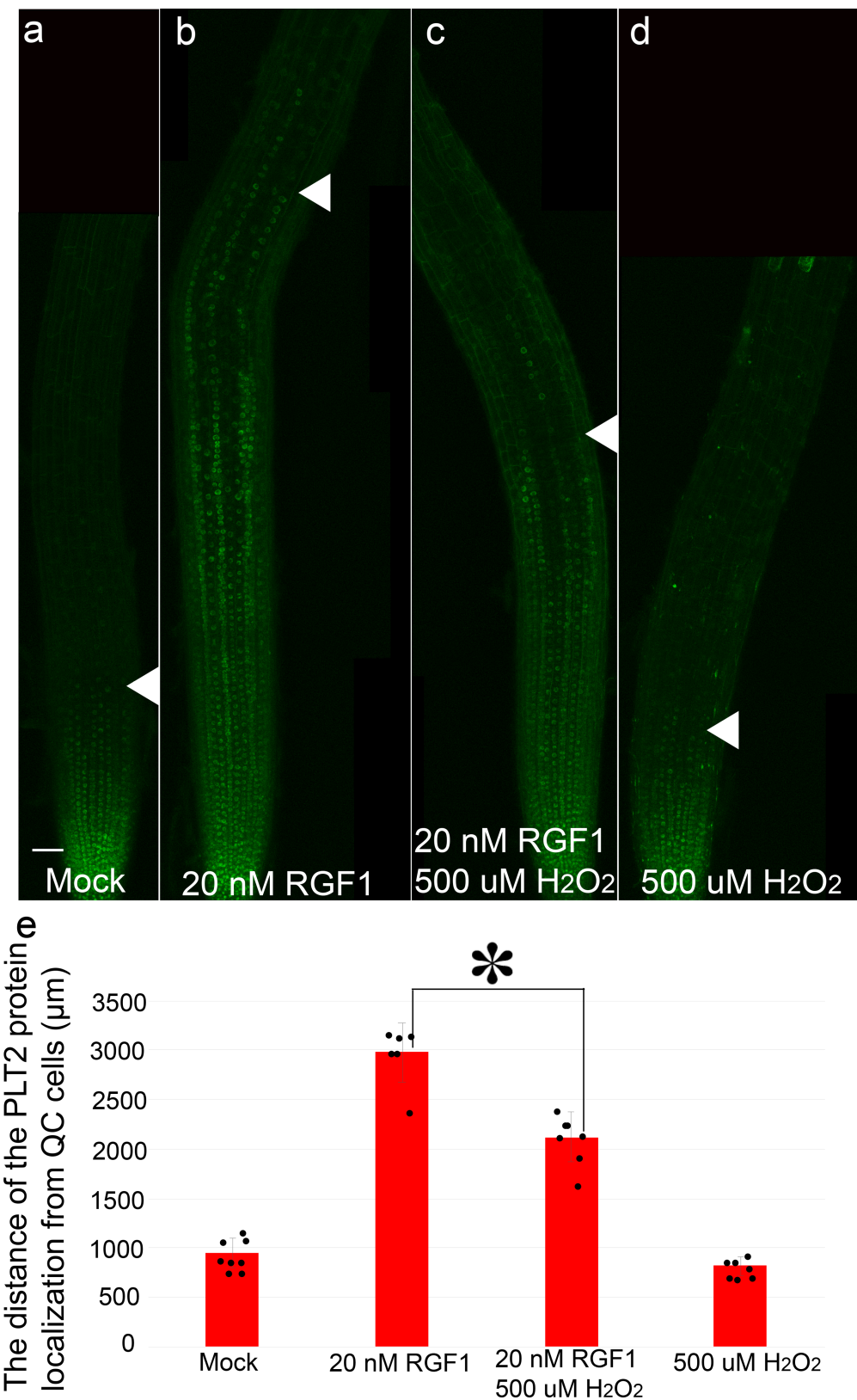
Extended Data Fig. 6 | Phenotype of *ritf* mutants. **a**, Root growth (in mm) of wild-type (Col), *ritf1-1* (CRISPR mutant) and *ritf1-2* (SALK line) seedlings from 4 to 8 days after germination ($n=21$ independent roots). **b**, Confocal images of wild-type, *ritf1-1* (CRISPR mutant) and *ritf1-2* (Salk line) roots stained with PI. **c**, Percentage increase (in which 100% is the number of cells in the mock-treated case) in the number of cells in the meristematic zone of wild-type, *ritf1-1* and *ritf1-2* roots 24 h after mock treatment or 5 nM RGF1 treatment ($n=7$ independent roots, $*P<5.4\times 10^{-6}$). **d**, Light microscope images of roots of wild-

type, *ritf1-3* and *ritf1-2* roots stained with NBT 24 h after treatment with 5 nM RGF1. Scale bars, 50 μ m. Blue arrowheads show the junction between the meristematic and elongation zones. **e**, Quantification of NBT staining intensity in the meristematic zone in wild-type, *ritf1-3* and *ritf1-2* roots after treatment with 5 nM RGF1 ($n=8$ independent roots; $*P<0.003$). Scale bars, 50 μ m. Blue and white arrowheads show the junction between the meristematic and elongation zones. Bar and line graphs show means. Error bars are \pm s.d. Dots indicate each data point. P values are calculated by two-sided Student's *t*-test.



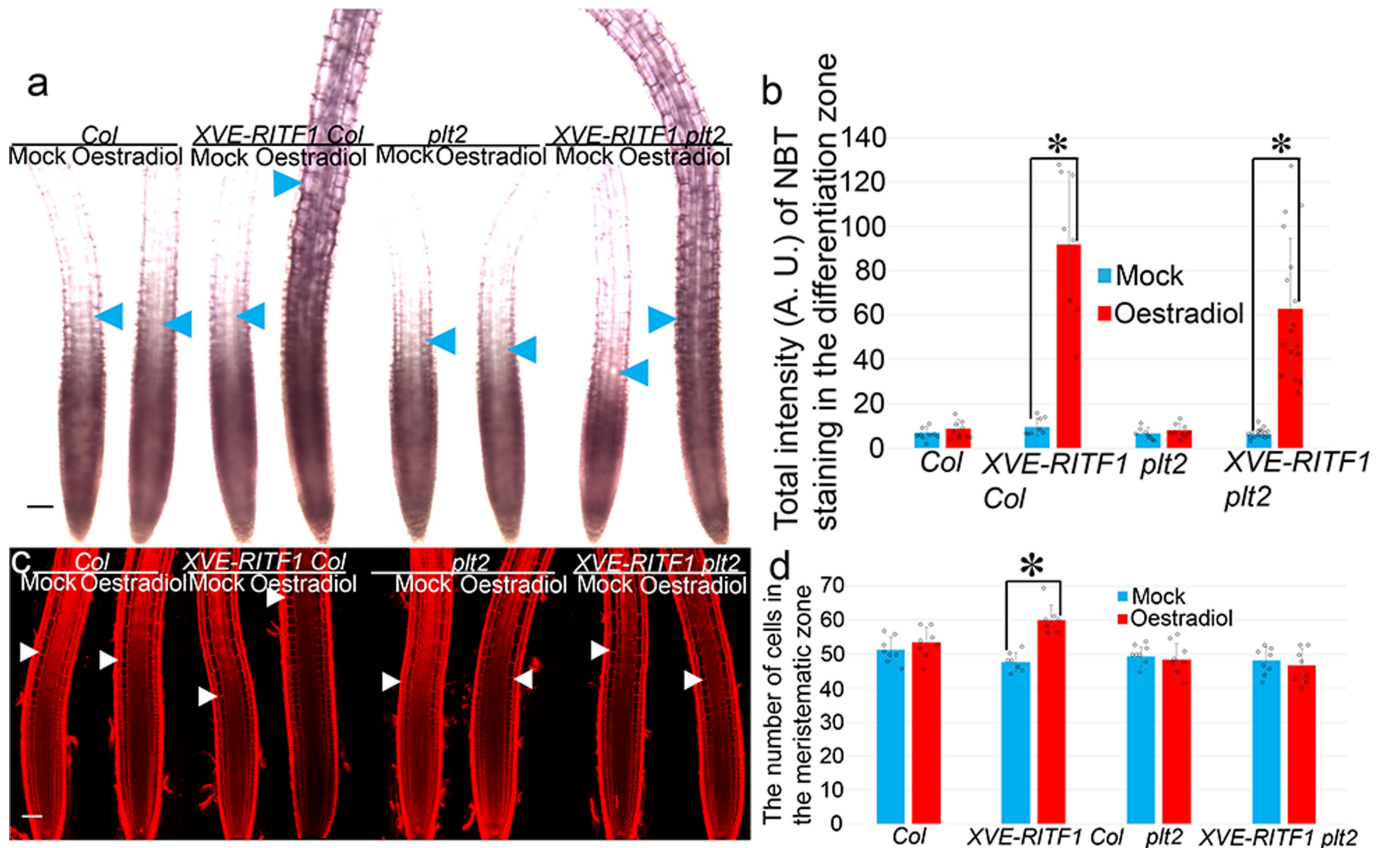
Extended Data Fig. 7 | Expression of *pPLT2-CFP* and *gPLT2-YFP* upon RGF1 treatment. **a, b**, Confocal images showing *pPLT2-CFP* expression (cyan; **a**) and *gPLT2-YFP* expression (green; **b**) 24 h after treatment with 20 nM RGF1. Red, PI staining. Scale bar, 50 μm . Arrow heads show the junction between the

meristematic and elongation zones. **c**, Extent (in μm) of *gPLT2-YFP* expression from quiescent-centre cells ($n=5$ independent roots; $P<2.5\times 10^{-13}$). Bar graphs show means. Error bars are \pm s.d. Dots indicate each data point. *P* values are calculated by two-sided Student's *t*-test.



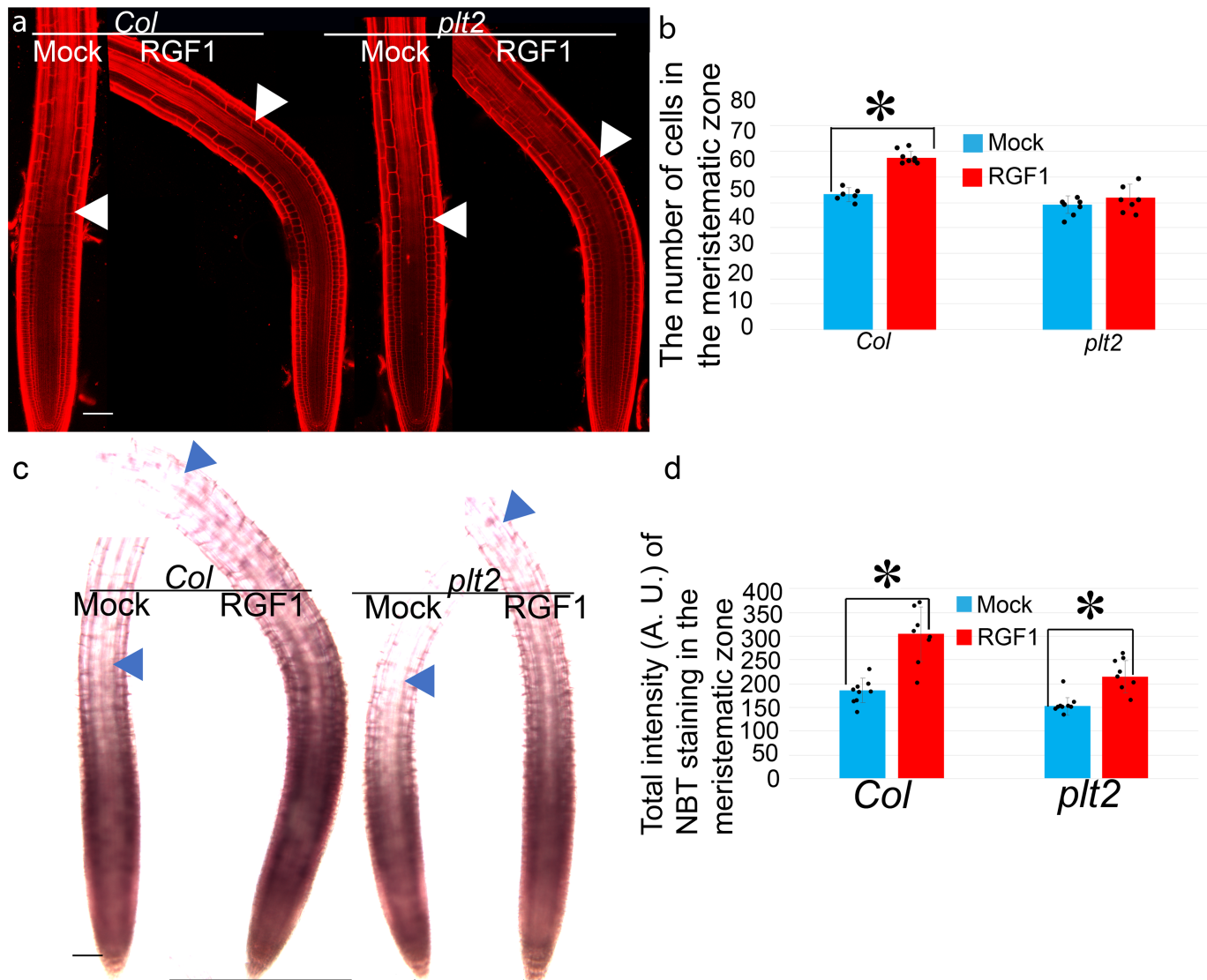
Extended Data Fig. 8 | Localization of PLT2 protein after RGF1 and/or H₂O₂ treatment. **a–d**, Confocal images showing gPLT2-YFP expression 24 h after treatment with water (mock), 20 nM RGF1, 20 nM RGF1 with 500 μM H₂O₂, or 500 μM H₂O₂. gPLT2-YFP seedlings were grown for seven days on MS agar plates before treatment. Scale bar, 50 μm. Arrowheads show the extent of gPLT2-YFP

expression. **e**, Distance (in μm) of PLT2 localization as measured from quiescent-centre cells ($n=6$, $*P<0.0002$). Bar graphs show means. Error bars are \pm s.d. Dots indicate each data point. P values calculated by two-sided Student's t -test.



Extended Data Fig. 9 | Phenotypes resulting from *RITF1* overexpression in *plt2* mutants. **a**, NBT-stained roots, with or without *XVE-RITF1* expression, in a wild-type or *plt2* background 24 h after treatment with water (mock) or 10 μ M oestradiol. **b**, Quantification of NBT staining intensity in the differentiation zone with or without *XVE-RITF1* in wild-type and *plt2* roots ($n=8$ independent roots; $*P<5.4\times10^{-6}$). **c**, Confocal images of PI-stained roots with or without *XVE-RITF1*, in a wild-type or *plt2* background, 24 h after mock treatment or

treatment with 10 μ M oestradiol. **d**, Number of cells in the meristematic zone, with or without *XVE-RITF1*, in wild-type and *plt2* roots 24 h after mock or 10 μ M oestradiol treatment ($n=7$ independent roots; $*P<4.3\times10^{-5}$). Scale bars, 50 μ m. White and blue arrowheads indicate the junction between the meristematic and elongation zones. Bar graphs show means. Error bars are \pm s.d. Dots indicate each data point. P values are calculated by two-sided Student's *t*-test.


Extended Data Fig. 10 | Phenotype of *plt2* roots upon RGF1 treatment.

a, Confocal images of PI-stained wild-type and *plt2* roots 24 h after treatment with water (mock) or 20 nM RGF1. Scale bar, 50 μ m. White arrowheads show junctions between the meristematic and elongation zones. **b**, Number of cells in the meristematic zone 24 h after mock or 5 nM RGF1 treatment ($n=6$ independent roots; $*P<4.9\times10^{-7}$). **c**, Light microscope images of roots from wild-type and *plt2* roots stained with NBT. Seedlings were grown on MS agar

plates for 7 days before treatment with water (mock) or 20 nM RGF1. **d**, Total intensity of NBT staining in the differentiation zone of wild-type and *plt2* roots 24 h after treatment with water (mock) or 20 nM RGF1 ($n=8$ independent roots; $*P<0.0003$). Scale bars, 50 μ m. White arrowheads show the junction between the meristematic and elongation zones. Bar graphs show means. Error bars are \pm s.d. Dots indicate each data point. P values are calculated by two-sided Student's *t*-test.

Corresponding author(s): Philip N. Benfey

Last updated by author(s): Oct 7, 2019

Reporting Summary

Nature Research wishes to improve the reproducibility of the work that we publish. This form provides structure for consistency and transparency in reporting. For further information on Nature Research policies, see [Authors & Referees](#) and the [Editorial Policy Checklist](#).

Statistics

For all statistical analyses, confirm that the following items are present in the figure legend, table legend, main text, or Methods section.

n/a Confirmed

- The exact sample size (n) for each experimental group/condition, given as a discrete number and unit of measurement
- A statement on whether measurements were taken from distinct samples or whether the same sample was measured repeatedly
- The statistical test(s) used AND whether they are one- or two-sided
Only common tests should be described solely by name; describe more complex techniques in the Methods section.
- A description of all covariates tested
- A description of any assumptions or corrections, such as tests of normality and adjustment for multiple comparisons
- A full description of the statistical parameters including central tendency (e.g. means) or other basic estimates (e.g. regression coefficient) AND variation (e.g. standard deviation) or associated estimates of uncertainty (e.g. confidence intervals)
- For null hypothesis testing, the test statistic (e.g. F , t , r) with confidence intervals, effect sizes, degrees of freedom and P value noted
Give P values as exact values whenever suitable.
- For Bayesian analysis, information on the choice of priors and Markov chain Monte Carlo settings
- For hierarchical and complex designs, identification of the appropriate level for tests and full reporting of outcomes
- Estimates of effect sizes (e.g. Cohen's d , Pearson's r), indicating how they were calculated

Our web collection on [statistics for biologists](#) contains articles on many of the points above.

Software and code

Policy information about [availability of computer code](#)

Data collection

No software was used.

Data analysis

DESeq2 v1.14.1; Bowtie2 v2.2.7; TopHat v2.1.1; Samtools v1.2; HTSeq v0.6.1, Fiji v2.0.0

For manuscripts utilizing custom algorithms or software that are central to the research but not yet described in published literature, software must be made available to editors/reviewers. We strongly encourage code deposition in a community repository (e.g. GitHub). See the Nature Research [guidelines for submitting code & software](#) for further information.

Data

Policy information about [availability of data](#)

All manuscripts must include a [data availability statement](#). This statement should provide the following information, where applicable:

- Accession codes, unique identifiers, or web links for publicly available datasets
- A list of figures that have associated raw data
- A description of any restrictions on data availability

All RNA-seq data in this study have been deposited in NCBI GEO with accession identifier GSE108730.

Field-specific reporting

Please select the one below that is the best fit for your research. If you are not sure, read the appropriate sections before making your selection.

- Life sciences Behavioural & social sciences Ecological, evolutionary & environmental sciences

For a reference copy of the document with all sections, see nature.com/documents/nr-reporting-summary-flat.pdf

Life sciences study design

All studies must disclose on these points even when the disclosure is negative.

Sample size	We used 3 biological replicates for RNA-seq, following the common practice in the field.
Data exclusions	No data were excluded.
Replication	We calculated gene-wise dispersion among biological replicates for RNA-seq data. The dispersion plot displayed typical pattern of RNA-seq.
Randomization	All samples for RNA-seq and measuring ROS and meristem size are randomly selected.
Blinding	For RNA-seq analysis, an investigator randomly collected samples and generated RNA-seq libraries. Another investigator did computational analysis. Our transcriptome analysis is completely blind.

Reporting for specific materials, systems and methods

We require information from authors about some types of materials, experimental systems and methods used in many studies. Here, indicate whether each material, system or method listed is relevant to your study. If you are not sure if a list item applies to your research, read the appropriate section before selecting a response.

Materials & experimental systems

n/a	Involved in the study
<input checked="" type="checkbox"/>	Antibodies
<input checked="" type="checkbox"/>	Eukaryotic cell lines
<input checked="" type="checkbox"/>	Palaeontology
<input checked="" type="checkbox"/>	Animals and other organisms
<input checked="" type="checkbox"/>	Human research participants
<input checked="" type="checkbox"/>	Clinical data

Methods

n/a	Involved in the study
<input checked="" type="checkbox"/>	ChIP-seq
<input checked="" type="checkbox"/>	Flow cytometry
<input checked="" type="checkbox"/>	MRI-based neuroimaging